Effect of composition on antiphase boundary energy in Ni_3Al based alloys: *Ab initio* calculations

O. I. Gorbatov,[1,2,3] I. L. Lomaev,[1,4,5] Yu. N. Gornostyrev,[1,4,5] A. V. Ruban,[2,6] D. Furrer,[7] V. Venkatesh,[7] D. L. Novikov,[8] and S. F. Burlatsky[8]

[1]*Institute of Quantum Materials Science, Ekaterinburg 620107, Russia*
[2]*Department of Materials Science and Engineering, KTH Royal Institute of Technology, SE-100 44 Stockholm, Sweden*
[3]*Nosov Magnitogorsk State Technical University, Magnitogorsk 455000, Russia*
[4]*Science for Technology LLC, Leninskiy pr-t 95, 119313 Moscow, Russia*
[5]*Institute of Metal Physics, Ural Division RAS, Ekaterinburg 620219, Russia*
[6]*Materials Center Leoben Forschung GmbH, A-8700 Leoben, Austria*
[7]*Pratt & Whitney, 400 Main Street, East Hartford, Connecticut 06108, USA*
[8]*United Technologies Research Center, 411 Silver Lane, East Hartford, Connecticut 06108, USA*

(Received 3 June 2015; revised manuscript received 23 May 2016; published 20 June 2016)

The effect of composition on the antiphase boundary (APB) energy of Ni-based $L1_2$-ordered alloys is investigated by *ab initio* calculations employing the coherent potential approximation. The calculated APB energies for the $\{111\}$ and $\{001\}$ planes reproduce experimental values of the APB energy. The APB energies for the nonstoichiometric γ' phase increase with Al concentration and are in line with the experiment. The magnitude of the alloying effect on the APB energy correlates with the variation of the ordering energy of the alloy according to the alloying element's position in the 3*d* row. The elements from the left side of the 3*d* row increase the APB energy of the Ni-based $L1_2$-ordered alloys, while the elements from the right side slightly affect it except Ni. The way to predict the effect of an addition on the $\{111\}$ APB energy in a multicomponent alloy is discussed.

DOI: 10.1103/PhysRevB.93.224106

I. INTRODUCTION

Nickel-based superalloys represent an important class of materials which have outstanding high-temperature strength and oxidation resistance [1,2]. They are widely used in aircraft and power-generation turbines and rocket engines, which work in high-temperature environments. Due to their high technological importance, these alloys have been attracting researchers' interest for several decades [2,3].

The strength of Ni-based superalloys originates from the presence of the ordered γ' (Ni_3Al-type structure) phase, which is distributed within the disordered fcc γ matrix [2,3]. High resistance to the plastic deformation of two phase γ/γ' alloys is caused by the need of the antiphase boundary (APB) ribbon formation when a single γ-phase $1/2\langle 110\rangle$ dislocation cuts a γ' particle in two-phase γ/γ' alloys. Thus, the APB energy is one of the most important parameters that determines the superdislocation structure [1,2,4,5], the mechanical behavior of the γ' phase, and the strength of the γ/γ' alloys.

Unfortunately, it is not possible to measure the APB energy directly. The most promising experimental technique is based on the measurement of the dissociation splitting distance of superpartial dislocations within the γ' phase followed by the estimate of the APB energy on the basis of the theoretical dislocation description (e.g., continual elasticity or Peierls-Nabarro model) [6–10]. For the measurement of the splitting distance, the weak-beam transmission electron microscopy is commonly used. It is, however, somewhat difficult to determine the exact orientation of superpartial dislocations within the lattice, which results in a significant spread in experimental values of APB energies.

The first theoretical estimation of the APB energy based on the simple central pair interatomic interactions model was proposed in Ref. [11]. This model was further developed in Refs. [12–15] in which an attempt was made to establish the relation between the APB energy and thermodynamic parameters of alloys such as mixing and ordering enthalpies (or ordering temperature). This approach reveals general trends in the family of Ni_3Al-type alloys. However, it does not provide a reliable value of the APB energy due to well-known limitations of the nearest-neighbor pair potential approximation in metallic alloys.

Atomistic calculations of APB energies were performed using various techniques. It was found that results of molecular dynamic simulations (see Ref. [16] and references therein) are very sensitive to details of approximations for interatomic potentials and contain uncontrollable errors. At the same time, theoretical methods based on first-principles calculations using density functional theory (DFT) are now becoming an efficient and accurate research tool permitting wide possibilities for modeling defects. The $\{111\}$ and $\{001\}$ APB energies of ordered $L1_2$ alloys were calculated using full potential methods [6,17,18] and Green's-function technique within the linear muffin-tin orbital method [19]. It was revealed that first-principles calculations predict APB energies in agreement with experiments when atomic relaxations near APB planes are taken into account [20]. However, previous *ab initio* calculations of the APB energy in Ni-based $L1_2$ alloys [6,17–21] have been performed for ferromagnetic or nonmagnetic states, while they are paramagnetic for all temperatures of interest ($T_{\mathrm{Curie}} = 41.5$ K for Ni_3Al).

Various experiments show that the APB energy is very sensitive to the alloy composition (stoichiometry deviation, alloying addition, etc.) [7,8,22,23]. According to Dimiduk *et al.* [24], the $\{001\}$ APB energy increases with Al content, but results by Yu *et al.* [25] show the opposite trend. Meanwhile, a study by Kruml *et al.* [8] confirms the results of Ref. [24]

showing an increase of both $\{001\}$ and $\{111\}$ APB energies along with Al content.

Despite the importance of the composition effect on APB energies, there are few theoretical studies of ternary and multicomponent systems [21,26–28]. In Ref. [28], a predictive approach to estimate the APB energy for the γ' phase as a function of its chemistry was proposed. It included a thermodynamic modeling and *ab initio* calculations of ordering energies in ternary Ni_3Al-based alloys. First-principles calculations of APB energies in the $\{111\}$ plane were performed in Refs. [21,26,27] for $Ni_3Al_{1-x}Z_x$ (Z = Ti, Nb, Ta) within the supercell approach with a quasirandom distribution of alloying elements at Al sites. According to Ref. [21], for all of these elements, the APB energy in the $\{111\}$ plane slightly increases with concentration of addition up to $x = 20$ at.% and decreases (at fixed concentration) in sequence Ti, Nb, and Ta.

Due to the absence of the unique ground-state structure, accurate energy calculations of random alloys require configurational averaging of energies. The technique, however, used in Refs. [21,26,27] did not provide reliable configuration statistics. An approach based on the cluster expansion and Monte Carlo method using first-principles total-energy calculations was recently proposed and allowed for studying the effect of Ti on APB energies [29]. One of the effective ways to solve this problem is to employ a single-site mean-field type of averaging, which, for instance, is done in the coherent potential approximation (CPA) [30] used for the electronic structure calculations of alloys. This makes the CPA-based technique attractive for investigations of the alloying effect on APB energies. In the present paper, the CPA-based approach is employed for direct calculations of $\{111\}$ and $\{001\}$ APB energies in binary $Ni_{3-x}Al_{1+x}$ and ternary $Ni_{3-x}Al_{1-y}Z_{x+y}$ alloys, in which Z is a $3d$ transition element (i.e., Z = Ti, V, Cr, Mn, Fe, Co, Cu). The obtained results allow for an identification of the alloying effect in the APB energy in $L1_2$-ordered Ni-based alloys and open a way to predict the APB energy for multicomponent systems.

II. METHODOLOGY

The *conservative* APB energy, ξ_{hkl}, for a crystal plane $\{hkl\}$ is postulated as the excess free energy (per unit area) due to the shift of one part of a crystal along a $\{hkl\}$ plane by the vector $\mathbf{b}$ ($\mathbf{b} = 1/2 < 110 >$). The temperature dependence of ξ_{hkl} is caused by the thermal expansion and the change of a free energy of an alloy as a result of different thermal excitations [31]. The vibrational entropy and the thermal electronic excitation contributions were calculated from first principles using the quasiharmonic approximation [32]. It was shown that the finite-temperature $\{001\}$ APB free energy was reduced approximately by 10% in the temperature range 0 to 300 K. The $\{111\}$ APB free energy was found to be practically independent of the temperature. The temperature dependence of APB energies was found experimentally to be small in Ref. [25] in which the temperature increase from 25 to 300 °C leads to the decrease of the $\{001\}$ APB energy by 3% and the increase of the $\{111\}$ APB energy by 7%. Therefore, the present study focuses on the alloying effect at the ambient temperature and neglects the entropy contribution. It is assumed that alloying elements are randomly distributed in the alloy and there is no segregation on the APB itself, which can be formed under certain conditions such as annealing. This corresponds to the *homogeneous* APB [27] that is related to the dislocation structure and the mobility at the ambient temperature. The effect of segregation on the thermodynamics of the $\{111\}$ APB was discussed in Ref. [33]. According to Refs. [34,35], the elements, which occupy the Al sublattice, segregate away from the $\{111\}$ and $\{001\}$ APBs.

For APB simulations in the $L1_2$ structure, the 48-atomic supercell was built by stacking 12 $\{111\}$ layers for the $\{111\}$ APB and the 32-atomic supercell was built by stacking 16 $\{001\}$ layers for the $\{001\}$ APB. As is shown in Refs. [21,36], such supercell sizes are large enough to avoid interactions between neighboring APBs. Due to periodic boundary conditions, the supercell contains two APBs, so the value of the APB energy has been calculated as

$$\xi_{hkl} = [E^{sc}(\{hkl\},\mathbf{b}) - E^{sc}(\{hkl\},0)]/2S. \quad (1)$$

Here, $E^{sc}(\{hkl\},\mathbf{b})$ and $E^{sc}(\{hkl\},0)$ are total energies of the supercells with and without APB, and S is the area of the antiphase boundary.

The magnetic and the atomic configurational disorders have been treated using the CPA [30], which accurately describes disordered systems in the single-site approximation. In this method, the real distribution of atoms in the alloy is represented by an effective medium with self-consistent parameters of the electron scattering. This approach gives a reliable way to model alloys with alloying elements randomly distributed in a particular sublattice. The paramagnetic state of the γ' phase has been considered using the disordered local moment (DLM) model [37]. This model treats spin-up ($\uparrow$) and spin-down ($\downarrow$) components for each magnetic element as randomly distributed.

In the case of deviation from the stoichiometric composition, the excess of Al or Ni was substituted into the opposite sublattice. For the ternary alloy modeling, solute atoms were randomly distributed between sublattices of the ordered γ' phase using the site preference of alloying elements, which was determined in a number of studies [3,38–44]. In Ni_3Al structure, Ti, V, Cr, and Mn atoms occupy the Al sublattice; Co and Cu occupy the Ni sublattice; and Fe can occupy both sublattices. The ternary addition Z was placed randomly in the Al and/or the Ni sublattice in $Ni_{3-x}Al_{1-y}Z_{x+y}$ alloy according to its site preference. Within the CPA, sites in Ni and Al sublattices are occupied by the mixture of atomic species Ni and Z, as well as Al and Z, with concentrations $c_{Ni} = 1 - x/3$, $c_{Z_{Ni}} = x/3$ and $c_{Al} = 1 - y$, $c_{Z_{Al}} = y$ for each sublattice accordingly. It should be noted that the actual distribution of alloying elements between sublattices depends on composition and temperature.

Electronic structure and total-energy calculations have been done by the exact muffin-tin orbitals (EMTO) method [45–47]. Atomic and magnetic disorders were introduced by applying CPA [30]. The accuracy of EMTO-CPA has been checked by locally self-consistent Green's-function (LSGF) calculations [48]. The LSGF method was also used to calculate screening parameters determining the contribution of screened Coulomb interactions to the one-electron potential V_i^{scr} of the alloy component i and to the total energy E_{scr} within the single-site

DFT formalism [49]:

$$V_i^{\mathrm{scr}} = -\alpha_{\mathrm{scr}} \frac{e^2 q_i}{s} \quad \text{and} \quad E_{\mathrm{scr}} = \frac{\beta_{\mathrm{scr}}}{2} \sum_i c_i q_i V_i^{\mathrm{scr}}. \qquad (2)$$

Here, e is the electron charge, s is the Wigner-Seitz radius, and q_i and c_i are the average net charge of the atomic sphere and the concentration of the ith alloy component, respectively. Screening constants were calculated for fixed alloy compositions. For example, the calculated screening constants for Ni_3Al are $\alpha_{\mathrm{scr}} = 0.68$ and $\beta_{\mathrm{scr}} = 1.10$.

EMTO-CPA total energies were calculated in the generalized gradient approximation (GGA) [50] using the full charge density formalism [45]. The multipole-moment correction in the atomic sphere approximation [51] was used. All self-consistent EMTO-CPA calculations were performed for the orbital momentum cutoff of $l_{\max} = 3$ for partial waves. The integration over the Brillouin zone was done using $18 \times 18 \times 4$ and $24 \times 24 \times 3$ grid of **k** points determined according to the Monkhorst-Pack scheme for 48-atomic and 32-atomic supercells, respectively [52]. Experimental values of lattice parameters of the Ni_3Al and ternary alloys at room temperature were used in the present calculations [53]. It should be noted that to estimate the effect of the lattice constant, EMTO-CPA calculations were performed with experimental and theoretical lattice parameters. Our calculations showed that the change of the lattice parameter of 0.4% did not affect our final conclusions.

To estimate the relaxation energy correction $\Delta\xi_{\mathrm{rel}}$, the APB energy difference between the relaxed and the unrelaxed states of ferromagnetic and nonmagnetic Ni_3Al was calculated with the 48-atomic and the 32-atomic supercells for the $\{111\}$ and $\{001\}$ APB by using the projector augmented wave (PAW) method [54] as implemented in the VASP code [55]. For three planes above and below the APB plane $\{hkl\}$, local lattice relaxations were performed by allowing displacements in the direction perpendicular to the APB plane only using the conjugate-gradient algorithm. This partial local relaxation gives the main contribution to $\Delta\xi_{\mathrm{rel}}$. Permitting the in-plane relaxation causes an undesirable distortion of a crystal that destroys the APB geometry. As was shown in Ref. [6], the shift of one part of a crystal in the $1/2 < 110 >$ direction (it corresponds to the so-called geometrical APB) moves atoms of adjacent crystal layers to positions which do not provide a local energy minimum. Since the true position of the energy minimum in Ni_3Al is only slightly shifted from its *geometrical* counterpart, we perform calculations for the latter APB that is a characteristic for the dislocation structure.

Ordering energies for Ni_3Al and ternary Ni_3Al-based alloys are calculated as the difference of the energies of ordered and random alloys with the same composition. In the case of ternary alloys, the alloying element is randomly distributed in a particular sublattice according to its site preference. Ordering energies in ternary Ni_3Al-based alloys were obtained by EMTO-CPA calculations, while an ordering energy in Ni_3Al was defined using both EMTO-CPA and PAW-VASP calculations. Random alloys for PAW-VASP calculations were modeled by a 108-atom $3 \times 3 \times 3$ supercell built upon a cubic fcc unit cell consisting of four atoms.

PAW-VASP calculations were performed using the GGA with the kinetic energy cutoff of 350 eV and using uniform $18 \times 18 \times 4$, $24 \times 24 \times 3$, and $6 \times 6 \times 6$ meshes of **k** points for 48-, 32-, and 108-atomic supercells, respectively. The convergence tolerance for the total energy was 10^{-6} eV/atom and 10^{-3} eV/Å for forces. The lattice constant of Ni_3Al in the ground state is 3.57 Å in the spin-restricted calculations, in agreement with the room-temperature experimental data [56]. Spin-polarized calculations show a similar result. This lattice constant was used in PAW-VASP calculations.

Values of $\Delta\xi_{\mathrm{rel}}$ for the $\{111\}$ and $\{001\}$ APB energies are found to be 70 and 14 mJ/m^2, correspondingly, in the nonmagnetic state. The relaxation correction energies depend weakly on the magnetic state of Ni (the difference of $\Delta\xi_{\mathrm{rel}}$ between nonmagnetic and ferromagnetic states does not exceed a few percent). Effects of the magnetic state as well as the alloying effect on the relaxation (discussed below) are small and the same value of $\Delta\xi_{\mathrm{rel}}$ was used for all considered cases.

III. RESULTS AND DISCUSSION

A. APB energies in $Ni_{3-x}Al_{1+x}$ alloy

Results of supercell EMTO-CPA calculations of APB energies for paramagnetic (DLM) binary $Ni_{3-x}Al_{1+x}$ alloys with the relaxation correction (calculated by PAW-VASP), $\Delta\xi_{\mathrm{rel}}$, are presented in Fig. 1 and Table I together with available experimental data and results of previous calculations. Table I shows that calculated APB energies are in reasonable agreement with experiments. They are within the range of the measured APB values. Slightly higher experimental values for the $\{001\}$ plane [references (A)–(D) in Fig. 1] could originate from the fact that the structure of the superdislocation in the $\{001\}$ plane is not coplanar. Therefore, the use of mechanical equilibrium conditions for describing the structure of the superdislocation leads to the underestimation of its width [5,10].

Calculations show that the APB energy for the paramagnetic state is about 10% lower than the one in the ferromagnetic state (see Fig. 1) for both $\{111\}$ and $\{001\}$ APB planes. The same effect of the magnetic order was reported in Ref. [20]. Note that the difference between APB energies for the ferromagnetic and paramagnetic states decreases with Al concentration increase. Meanwhile, the APB energies in nonmagnetic calculations are found to be close to paramagnetic results. For the $\{111\}$ APB, the relaxation has a larger effect on the energy than the magnetic state effect. At the same time, for the $\{001\}$, both of the APB contributions are comparable.

As can be seen in Fig. 1, the APB energy is very sensitive to Al concentration: ξ_{001} changes by up to 50% with only a 2.5% variation in the composition. In the Ni-rich γ' phase, the presence of Ni in the Al sublattice leads to a decrease of both $\{111\}$ and $\{001\}$ APB energies. This is consistent with earlier theoretical investigations [26]. Simultaneously, it was found that in the Al-rich γ' phase (when Al is present in the Ni sublattice), both the APB energies are increased and this effect is more pronounced for the $\{001\}$ APB. Both $\{111\}$ and $\{001\}$ calculated APB energies are in agreement

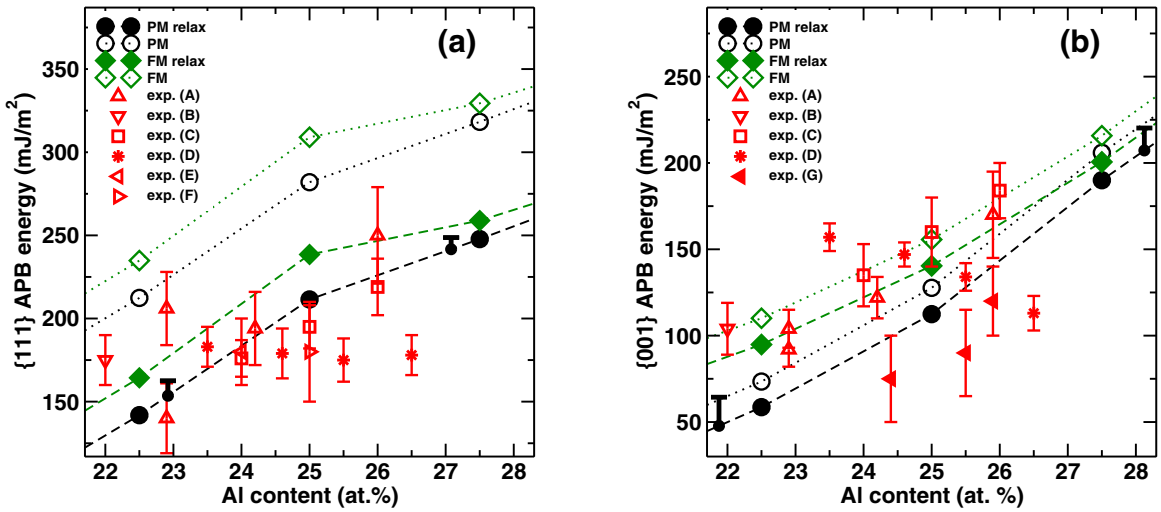

FIG. 1. Effect of deviation from stoichiometry on APB energies. Open circles and boxes (dashed lines) correspond to results of ferromagnetic and paramagnetic EMTO-CPA calculations. Closed circles and boxes (solid lines) correspond to EMTO-CPA results with the relaxation correction for Ni_3Al. The circles with bars show the variations due to local atomic relaxations in Ni_3Al-based alloys. The effect of different alloy configurations on the relaxation correction dispersion is indicated by error bars. Experimental data are from Dimiduk *et al.* [24] (A), Karnthaler *et al.* [7] (B), Kruml *et al.* [8] (C), Yu *et al.* [25] (D), Hemker and Mills [9] (E), Veyssiere *et al.* [57] (F), and Douin and Veyssire [58] (G).

TABLE I. APB energies in $Ni_{3-x}Al_{1+x}$ (mJ/m^2).

(*hkl*)	Al (at.%)	Present calculations	Experiment [Ref.]	Previous calculations
{111}	27.5	247		
	26.5		178 ± 12 [25]	
	26		219 ± 17 [8]	
	25.9		250 ± 29 [24]	
	25.5		175 ± 13 [25]	
	25	211	195 ± 13 [8], 180 ± 30 [57]	210 [6], 252 [16], 240 [19], 181 [21], 188 [61], 179 [36], 223 [60], 177 [20]
	24.6		179 ± 15 [25]	
	24.2		194 ± 22 [24]	
	24		176 ± 11 [8]	
	24		180 ± 20 [9]	
	23.5		183 ± 12 [25]	
	22.9		206 ± 22 [24], 140 ± 21 [24,59]	
	22.5	142		
	22		175 ± 15 [7]	
{001}	27.5	190		
	26.5		113 ± 10 [25]	
	26		184 ± 16 [8]	
	25.9		170 ± 25 [24], 120 ± 20 [58]	
	25.5		134 ± 8 [25]; 90 ± 5 [58]	
	25	112	160 ± 20 [8], 140 ± 14 [57]	80[16], 137 [19], 107 [21], 96 [36], 82 [32]
	24.6		143 ± 7 [25]	
	24.4		75 ± 25 [58]	
	24.2		122 ± 12 [24]	
	24		135 ± 18 [8]	
	23.5		157 ± 8 [25]	
	22.9		104 ± 11 [24], 92 ± 10 [24,59]	
	22.5	59		
	22		104 ± 15 [7]	

with the most reliable experimental data [points (A) and (C) in Fig. 1] and show a general trend of the APB energy to increase with Al concentration [8,24]. It should be noted that at the same time, experimental results in Ref. [25] [points (D) in Fig. 1] for the {001} APB energy are in contradiction with Refs. [8,24,57] and show the opposite trend. Keeping in mind that experimental data on the APB energy contain errors, the experimental and calculated results are in reasonable agreement.

Results presented in Fig. 1 are obtained in the approximation that the relaxation correction does not depend on composition of alloys. To estimate the effect of deviation from the stoichiometry on the value of $\Delta\xi_{\rm rel}$, the APB energy of the $Ni_{3-x}A_{1+x}$ alloy was calculated by using the PAW-VASP method with relaxations as in the case of a stoichiometric alloy for $x = \pm 2.08$ at.% for the {111} plane and $x = \pm 3.125$ at.% for the {001} plane. Because obtained results depended on specific distribution of chemical components, calculations were done for several particular placements of excess atoms in corresponding sublattices. Results of these calculations are shown in Fig. 1 at corresponding concentrations of Al. As can be seen within the considered concentration interval, the effect of composition on the relaxation correction $\Delta\xi_{\rm rel}$ appears to be small. The increase of a lattice constant due to the thermal expansion leads to a reduction in the effect of relaxations on the APB energy. Thus, the CPA-based approach provides a reliable description of the *homogeneous* APB energy in spite of the simplified relaxation treatment.

B. APB energies in ternary Ni_3Al-Z alloy

Figure 2 presents the calculated APB energies in ternary Ni_3Al-based alloys with 2.5 at.% of 3*d* dopants. The solute atoms were distributed between sublattices according to their site-preference energy (see Sec. II). The relaxation correction for the stoichiometric Ni_3Al, $\Delta\xi_{\rm rel}$, was taken into account as in the previous section. It was found that the 3*d* alloying elements, such as Ti, V, and Cr, which occupy the Al sublattice, increase the APB energy for both {111} and {001} planes, while Mn has little effect on the APB energy for the {001} plane and decreases it for {111}. While Fe atoms occupy both the Al and Ni sublattices, Cu and Co atoms occupy only the Ni sublattice. They do not produce a strong effect on both {111} and {001} APB energies. Substitution of Al by Ni, however, strongly lowers both of the APB energies.

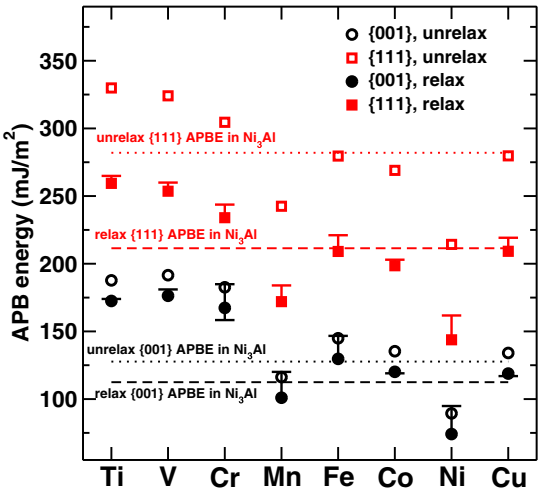

FIG. 2. *Ab initio* calculated APB energies in the {111} and {001} planes of Ni_3Al alloyed by 2.5 at.% of 3*d* elements without (unfilled square and circle) and with (filled square and circle) the local relaxation corrections for Ni_3Al. The effects of local relaxations for ternary alloys on the relaxation correction are indicated by error bars. Calculated APB energies in the {111} and {001} planes of Ni_3Al are shown by horizontal lines. Circles and squares with bars correspond to the effect of atomic local relaxations in Ni_3Al-based alloys.

To estimate the effect of alloying elements on $\Delta\xi_{\rm rel}$, the APB energy of ternary alloys was calculated by using the PAW-VASP method taking into account partial local atomic relaxations (see above for details). Calculations were done for several particular placements of ternary elements in corresponding sublattices with concentrations 2.08 at.% for the {111} plane and 3.125 at.% for the {001} plane. These concentrations are the closest to 2.5 at.%, which can be implemented within the used supercell geometries. Results of these calculations are shown in Fig. 2. As can be seen for the considered concentration, the error due to an *ad hoc* added relaxation and, consequently, the effect of ternary additions on the relaxation correction $\Delta\xi_{\rm rel}$ appear to be small for all elements except Cr, Mn, Fe, and Ni. Among these elements, only Cr is present in large concentrations in modern superalloys. In this case, the error may be more significant for larger concentrations and the employed method provides only qualitative conclusions. For other alloying elements, the use of the relaxation correction $\Delta\xi_{\rm rel}$ for stoichiometric Ni_3Al gives reliable results. Thus, this approximation can be considered as a reasonable one for the assessment of APB energies in ternary Ni_3Al-based alloys.

Figure 3 shows dependencies of APB energies calculated by EMTO-CPA with the relaxation correction in ternary Ni_3Al-based alloys as a function of an addition concentration. The variation of the APB energy in the γ' phase is mostly linear with the concentration of alloying elements up to 10 at.% with the exception of Cr addition. As in the case of the deviation from stoichiometry, the effect of the alloying addition on the APB energy is stronger for the {001} plane [cf. Figs. 3(a) and 3(b)], which is also reported for V in Ref. [24].

Results for Ti are in satisfactory agreement with previous calculations [21,26–28,36] for both APB planes and with the experiments [62,63]. The effect of V alloying was found to be similar. The increase of APB energies due to alloying by Ti and V is expected because both additions increase the stability of the γ' phase [2,22]. The Cr addition results in the nonmonotonic dependence of the APB energy on the concentration. With a small addition of Cr up to 5 at.%, APB energies increase in a manner similar to that of Ti and V. At the same time, the further increase of Cr content in the γ' phase leads to a substantial decrease of APB energies. This behavior of APB energies distinguishes Cr among other alloying elements and correlates with the nonmonotonicity of the enthalpy of the formation of Ni-rich Ni-Cr alloys [64]. The nonmonotonic dependence of the APB energy in the case of Cr is unclear and requires further study. It should be noted that our result for ξ_{111} at 10 at.% Cr is close to that in Ref. [28].

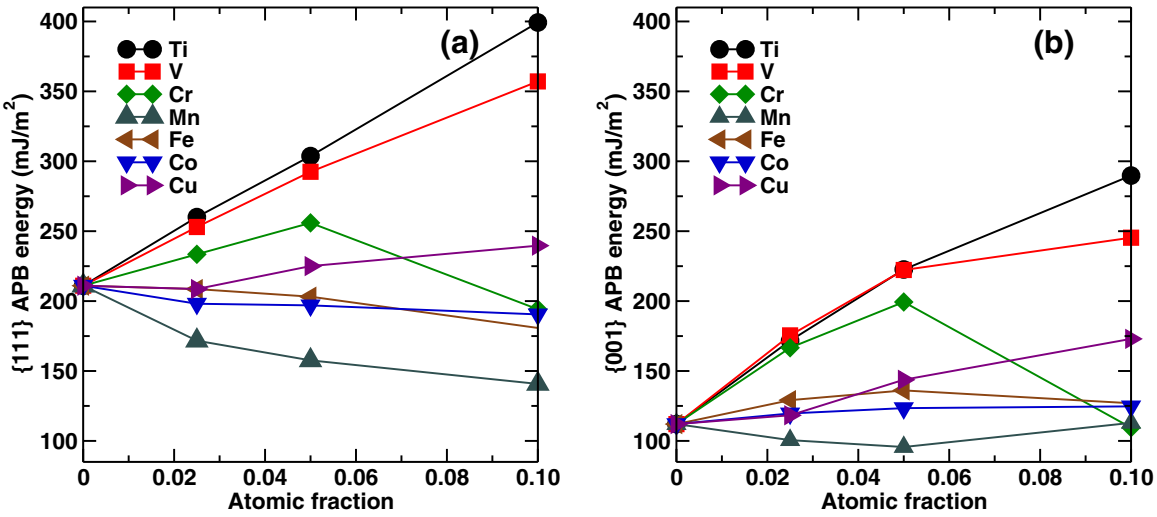

FIG. 3. Calculated APB energies in the (a) {111} and (b) {001} planes of Ni_3Al alloyed by 3*d* elements. The composition of ternary alloys $Ni_{3-y}Al_{1-x}Z_{x+y}$ has been chosen following sublattice occupation of alloying elements. $y = 0$ for Ti, V, Cr, Mn; $x = 3y$ for Fe; $y = 0$ for Co, Cu. Results are obtained by EMTO-CPA, taking into account the local relaxation for Ni_3Al from PAW-VASP calculations.

Finally, the magnetic effect will be discussed. It should be noted that APB energies in paramagnetic and nonmagnetic Ni_3Al are close to each other because it is a weak ferromagnet. At the same time, other alloying elements can exhibit quite different local magnetic behavior in Ni_3Al due to their magnetic properties and, in particular, the ability to keep local magnetic moments in the paramagnetic state (it can also be induced by spin fluctuations, but such effects are neglected here since the high-temperature state is not considered). For instance, Mn, Fe, and Co exhibit remarkably different effects on the APB energy in nonmagnetic and paramagnetic calculations, which are also known to increase the Curie temperature of Ni_3Al [65]. In particular, the {111} and {001} APB energies of the γ' phase containing 2.5% Mn are larger by 19% and 35%, respectively, in nonmagnetic than in paramagnetic calculations. In the case of Co and Fe, the difference between nonmagnetic and paramagnetic calculations is much smaller and does not exceed 5%.

C. Relation between APB energy and ordering energy

To understand trends in the APB energy caused by alloying elements, we calculated the ordering energy E_{ord} of ternary alloys. This is defined as the energy difference between the ordered alloy with the alloying element randomly distributed in a particular sublattice and a completely random alloy configuration with the same composition. The ordering energies for Ni_3Al and Ni_3Al-based alloys were calculated at the room-temperature lattice constant. The ordering energy for Ni_3Al has been found to be -0.13 eV/atom by EMTO-CPA without atomic relaxations in the paramagnetic (DLM) state, which is in line with previously calculated results [66]. This is in agreement with the result -0.12 eV/atom and -0.15 eV/atom obtained by nonmagnetic PAW-VASP supercell calculations with and without atomic relaxations.

The effect of alloying on E_{ord} and the APB energies ξ_{111} and ξ_{001} is presented in Fig. 4 as a function of a solute element position in the 3*d* row. It should be noted that Fig. 4 shows only a chemical contribution to the ordering and APB energies (without relaxations). As can be seen in Fig. 4, the variation of the APB energy, ξ_{111}, for alloying elements with concentration of 2.5% correlates very well with the ordering energy E_{ord} along the 3*d* row, although such a correlation worsens with alloying concentrations. For solutes from Ti to Mn which occupy the Al sublattice, E_{ord} and ξ_{111} decrease when the number of valence electrons increases. For solutes from Fe to Cu occupying Ni or both Ni and Al sublattices, these values show only a slight variation with the number of valence electrons. Ni addition in the Al sublattice is an exception in that it results in a sharp drop of both E_{ord} and ξ_{111} energies. This reflects the sensitivity of the APB energy to the stoichiometry variation in Ni-rich compositions.

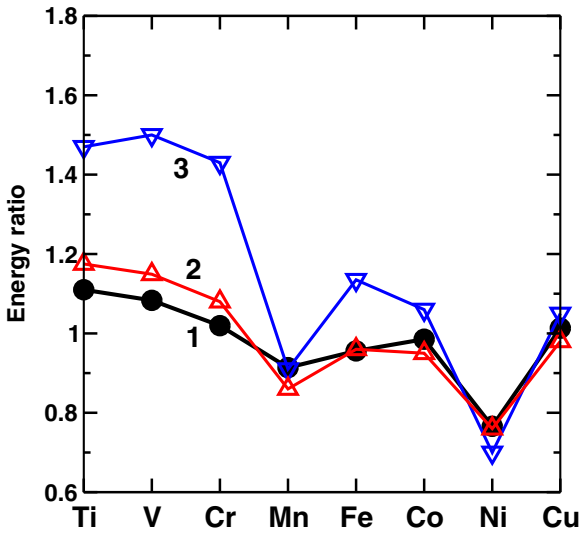

FIG. 4. Calculated ratio of the ordering energy of ternary alloys to the ordering energy of stoichiometric Ni_3Al, $E_{ord}/E_{ord}^{Ni_3Al}$ (curve 1), and ratios of APB energies of ternary alloy and Ni_3Al, $\xi_{111}/\xi_{111}^{Ni_3Al}$ and $\xi_{001}/\xi_{001}^{Ni_3Al}$ (curve 2 and 3, respectively), for 3*d* solutes. The concentration of alloying elements is 2.5 at.%.

The correlation between the APB energy ξ_{111} and the ordering energy $E_{\rm ord}$ is not surprising and is expected within the quasichemical approximation for the alloy model when the nearest-neighbor interatomic interactions dominate. Indeed, the ordering energy for A_3B of a completely ordered $L1_2$ alloy is

$$E_{\rm ord}^{L1_2} = -\frac{3}{16}(2V_1 - 3V_2 + 4V_3 - \cdots), \quad (3)$$

while $\{111\}$ and $\{001\}$ APB energies are [13]

$$\xi_{111} = \frac{1}{a^2\sqrt{3}}(V_1 - 3V_2 + 4V_3 - \cdots), \quad (4)$$

$$\xi_{001} = \frac{1}{a^2}(-V_2 + 4V_3 - \cdots), \quad (5)$$

where V_i is the effective interaction energy for the ith coordination sphere.

As is suggested in Ref. [14], the alloying element modifies values of effective interactions, so $V_i \to \tilde{V}_i$. This is the major effect at small concentrations. In this case, the ratio is $\xi_{111}/\xi_{111}^{\rm Ni_3Al} \approx E_{\rm ord}/E_{\rm ord}^{\rm Ni_3Al} \approx \tilde{V}_1/V_1$ if the nearest-neighbor interaction V_1 dominates. Note that Eqs. (4) and (5) neglect the atomic relaxation contribution which is essential for the $\{111\}$ plane (see Fig. 1). Nevertheless, the ratios $\xi_{111}/\xi_{111}^{\rm Ni_3Al}$ and $E_{\rm ord}/E_{\rm ord}^{\rm Ni_3Al}$ show a good correlation with the alloying element position in the $3d$ row. It means that the effect of alloying on ξ_{111} can be understood from the variation of the ordering energy which can be easily obtained from *ab initio* calculations. At the same time, for the $\{001\}$ plane, there is no pronounced correlation between APB and ordering energies (see Fig. 4) because the effective interaction energy V_1 is not included in Eq. (5). Thus, direct *ab initio* calculations of the $\{001\}$ APB energy are necessary.

IV. SUMMARY

The composition effect on the APB energy in Ni_3Al-based alloys has been investigated using *ab initio* modeling. The employed approach includes CPA-DFT calculations of the alloy energy variations due to the APB presence with randomly distributed substitute atoms in specific sublattices. It was assumed that there was no atomic segregation on the APB itself and there was neglected thermal entropy contributions to the APB energy. This corresponds to the *homogeneous* APB [27] formation, which is a controlling factor in the resistance to plastic flow in two-phase γ/γ' alloys. A contribution to the APB energy from local atomic relaxations has been accounted for with the relaxation correction for Ni_3Al, which is calculated by the PAW method. The use of the relaxation correction $\Delta\xi_{\rm rel}$ for stoichiometric Ni_3Al gives reliable results not only for nonstoichiometric but also for Ni_3Al alloyed by chemical elements, which are contained in the $\gamma\prime$ phase of Ni-based superalloys in a small amount and/or an effect of which on the $\Delta\xi_{\rm rel}$ is small, such as, for example, Ti and Co.

In spite of using simplification, this approach provides a reliable description of the alloy composition effect on the APB energy in Ni_3Al-based alloys. The calculated APB energies in nonstoichiometric $Ni_{3-x}Al_{1+x}$ alloys are in agreement with available experiments. This indicates that the employed approximations are quite reasonable. The obtained results show a general trend: the increase of the APB energy with Al concentration. The paramagnetic and nonmagnetic calculations of the APB energy give similar results. At the same time, ferromagnetic calculations overestimate both $\{111\}$ and $\{001\}$ APB energies.

Ternary additions, such as Ti, V, and Cr, which occupy the Al sublattice, increase the APB energy for both the $\{111\}$ and $\{001\}$ planes, while Mn has a little effect on the APB energy for the $\{001\}$ plane and decreases the energy for $\{111\}$. Co, Cu, and Fe, which occupy Ni or both sublattices, slightly affect both the $\{111\}$ and $\{001\}$ APB energies. The variation of the APB energy in the γ' phase is mostly linear with the concentration of Ti and V, which has the largest effect among $3d$ alloying elements. An exceptional and interesting case is that of Cr alloying, which leads to the nonmonotonic concentration dependence of ξ_{hkl}. The reasons for this behavior call for further investigations.

To summarize, the results of our calculations reveal trends in a variation of homogeneous APB energy ξ_{hkl} in Ni_3Al alloyed by $3d$ elements and pave a way for predicting the alloying effect on the APB energy in the $\{111\}$ plane based solely on the ordering energy calculation. It should be noted that the APB energy for Ni_3Al alloyed by $3d$ elements correlates with the ordering energy of these alloys. The approach that combines thermodynamic modeling [using the calculation of phase diagrams (CALPHAD)-based methods] and *ab initio* calculated ordering and mixing energies has been recently used in Ref. [28]. As is shown, CALPHAD methods have strong limitations due to the requirement of a high degree of extrapolation in the metastable phase region and first-principles calculations are necessary. The CPA-DFT approach with the atomic relaxation correction provides a reliable way for estimation of APB energies in ternary alloys. This approach can be easily extended to multicomponent alloys. It will provide the ability to predict the impact of substitutional additions in the ordered γ' phases on the dislocation motion, and subsequently, mechanical properties of multicomponent γ/γ' alloys.

[1] D. P. Pope, in *Physical Metallurgy*, edited by R. W. Cahn and P. Haasen (Elsevier, Amsterdam, 1996), Vol. III.

[2] R. C. Reed, *Superalloys. Fundamentals and Applications* (Cambridge University Press, Cambridge, 2006).

[3] G. Sauthoff, *Intermetallics* (VCH Verlagsgesellschaft, Weinheim, 1995).

[4] B. H. Kear and H. B. F. Wilsdorf, Trans. AIME **224**, 382 (1962).

[5] V. Paidar, D. P. Pope, and V. Vitek, Acta Metall. **32**, 435 (1984).

[6] O. N. Mryasov, Yu. N. Gornostyrev, M. van Schilfgaarde, and A. J. Freeman, Acta Mater. **50**, 4545 (2002).

[7] H. P. Karnthaler, E. Th. Mühlbacher, and C. Rentenberger, Acta Mater. **44**, 547 (1996).

[8] T. Kruml, E. Conforto, B. Lo Piccolo, D. Caillard, and J. L. Martin, Acta Mater. **50**, 5091 (2002).
[9] K. J. Hemker and M. J. Mills, Philos. Mag. A **68**, 305 (1993).
[10] *Dislocations in Solids. $L1_2$ Ordered Alloys*, edited by F. R. N. Nabarro and M. S. Duesbery (Elsevier, Amsterdam, 1996), Vol. 10.
[11] P. A. Flinn, Trans. AIME **218**, 145 (1960).
[12] D. J. Crudden, B. Raeisinia, N. Warnken, and R. C. Reed, Metall. Mater. Trans. A **44**, 2418 (2013).
[13] G. Inden, S. Bruns, and H. Ackermann, Philos. Mag. A **53**, 87 (1986).
[14] A. P. Miodownik and N. Saunders, *Applications of Thermodynamics in the Synthesis and Processing of Materials*, edited by P. Nash and B. Sundman (TMS, Warrendale, PA, 1995).
[15] F. Kral, P. Schwander, B. Schönfeld, and G. Kostorz, Mater. Sci. Eng. A **234-236**, 351 (1997).
[16] Y. Mishin, Acta Mater. **52**, 1451 (2004).
[17] A. T. Paxton, *Electron Theory in Alloy Design*, edited by D. G. Pettifor and A. H. Cottrell (The Institute of Materials, London, 1992).
[18] C. L. Fu, Y.-Y. Ye, and M. H. Yoo, *High-Temperature Ordered Intermetallic Alloys V*, edited by I. Baker *et al.* (Materials Research Society, Pittsburgh, 1993).
[19] N. M. Rosengaard and H. L. Skriver, Phys. Rev. B **50**, 4848 (1994).
[20] V. R. Manga, J. E. Saal, Y. Wang, V. H. Crespi, and Z.-K. Liu, J. Appl. Phys. **108**, 103509 (2010).
[21] M. Chandran and S. K. Sondhi, Model. Simul. Mater. Sci. Eng. **19**, 025008 (2011).
[22] N. F. Stoloff, Int. Mater. Rev. **34**, 153 (1989).
[23] D. M. Dimiduk, J. Phys. III **1**, 1025 (1991).
[24] D. M. Dimiduk, A. W. Thompson, and J. C. Williams, Philos. Mag. A **67**, 675 (1993).
[25] H. F. Yu, I. P. Jones, and R. E. Smallman, Philos. Mag. A **70**, 951 (1994).
[26] K. V. Vamsi and S. Karthikeyan, *Superalloys*, edited by E. S. Huron *et al.* (TMS, Warrendale, 2012).
[27] K. V. Vamsi and S. Karthikeyan, MATEC Web Conf. **14**, 11005 (2014).
[28] D. J. Crudden, A. Mottura, N. Warnken, B. Raeisinia, and R. C. Reed, Acta Mater. **75**, 356 (2014).
[29] R. Sun and A. van de Walle, CALPHAD **53**, 20 (2016).
[30] P. Soven, Phys. Rev. **156**, 809 (1967); D. W. Taylor, *ibid.* **156**, 1017 (1967).
[31] A. J. Skinner, J. V. Lilli, and J. Q. Broughton, Model. Simul. Mater. Sci. Eng. **3**, 359 (1995).
[32] V. R. Manga, S. L. Shang, W. Y. Wang, Y. Wang, J. Liang, V. H. Crespic, and Z. K. Liu, Acta Mater. **82**, 287 (2015).
[33] M. Sluiter, Y. Hashi, and Y. Kawazoe, Comput. Mater. Sci. **14**, 283 (1999).
[34] H. P. Wang, M. Sluiter, and Y. Kawazoe, Mater. Trans. **40**, 1301 (1999).
[35] H. P. Wang, M. Sluiter, and Y. Kawazoe, Mater. Trans. **42**, 407 (2001).
[36] X.-X. Yu and C.-Y. Wang, Philos. Mag. **92**, 4028 (2012).
[37] B. L. Gyorffy, A. J. Pindor, J. B. Stauton, G. M. Stocks, and H. Winter, J. Phys. F **15**, 1337 (1985).
[38] M. H. F. Sluiter, M. Takahashi, and Y. Kawazoe, Acta Mater. **44**, 209 (1996).
[39] A. V. Ruban and H. L. Skriver, Phys. Rev. B **55**, 856 (1997).
[40] C. Jiang, D. J. Sordelet, and B. Gleeson, Acta Mater. **54**, 1147 (2006).
[41] C. Jiang and B. Gleeson, Scr. Mater. **55**, 433 (2006).
[42] C. Booth-Morrison, Z. Mao, R. D. Noebe, and D. N. Seidman, Appl. Phys. Lett. **93**, 033103 (2008).
[43] M. Chaudhari, A. Singh, P. Gopal, S. Nag, G. B. Viswanathan, J. Tiley, R. Banerjee, and J. Du, Philos. Mag. Lett. **92**, 495 (2012).
[44] A. V. Ruban, V. A. Popov, V. K. Portnoi, and V. I. Bogdanov, Philos. Mag. **94**, 20 (2014).
[45] L. Vitos, *Computational Quantum Mechanics for Materials Engineers: The EMTO Method and Applications* (Springer-Verlag, London, 2007).
[46] L. Vitos, Phys. Rev. B **64**, 014107 (2001).
[47] L. Vitos, I. A. Abrikosov, and B. Johansson, Phys. Rev. Lett. **87**, 156401 (2001).
[48] I. A. Abrikosov, S. I. Simak, B. Johansson, A. V. Ruban, and H. L. Skriver, Phys. Rev. B **56**, 9319 (1997).
[49] A. V. Ruban, S. I. Simak, P. A. Korzhavyi, and H. L. Skriver, Phys. Rev. B **66**, 024202 (2002).
[50] J. P. Perdew, K. Burke, and M. Ernzerhof, Phys. Rev. Lett. **77**, 3865 (1996).
[51] H. L. Skriver and N. M. Rosengaard, Phys. Rev. B **43**, 9538 (1991).
[52] H. J. Monkhorst and J. D. Pack, Phys. Rev. B **13**, 5188 (1972).
[53] Y. Mishima, S. Ochial, and T. Suzuki, Acta Metall. **33**, 1161 (1985).
[54] P. E. Blöchl, Phys. Rev. B **50**, 17953 (1994).
[55] G. Kresse and D. Joubert, Phys. Rev. B **59**, 1758 (1999).
[56] P. V. M. Rao, S. V. Suryanaryana, K. S. Murthy, and S. V. N. Naidu, J. Phys. Condens. Matter **1**, 5357 (1989).
[57] P. Veyssiere, J. Douin, and P. Beauchamp, Philos. Mag. A **51**, 469 (1985).
[58] J. Douin and P. Veyssire, Philos. Mag. A **64**, 807 (1991).
[59] Annealed 1 h at 700 °C.
[60] J. Wang and H. Sehitoglu, Intermetallics **52**, 20 (2014).
[61] A. T. Paxton and Y. Q. Sun, Philos. Mag. A **78**, 85 (1998).
[62] A. Korner, Philos. Mag. A **58**, 507 (1988).
[63] T. Kawabata, D. Shindo, and K. Hiraga, Mater. Trans. JIM **33**, 565 (1992).
[64] M. Rahaman, B. Johansson, and A. V. Ruban, Phys. Rev. B **89**, 064103 (2014).
[65] N. I. Kourov, S. Z. Nazarova, A. V. Korolev, Y. A. Dorofeev, N. V. Volkova, and E. V. Belozerov, Phys. Met. Metallogr. **110**, 1 (2010).
[66] M. Sluiter, P. E. A. Turchi, F. J. Pinski, and G. M. Stocks, J. Phase Equilib. **13**, 605 (1992).